PAPER • OPEN ACCESS

Highly Improved Thermionic Energy Converter

View the article online for updates and enhancements.

Highly Improved Thermionic Energy Converter

D. K. De[a,b], O. C. Olawole[a,e], S. O. Oyedepo[c], E. S. Joel[a], O. F. Olawole[d], M. E. Emetere[a], [a]Omeje M and U I Ikono[a] and H M Nguyen[e,f]

[a]Department of Physics, Covenant University, Ota, Ogun State, Nigeria. [b]Sustainable Green Power Technology, Texas, USA. [c]Department of Mechanical Engineering, Covenant University, Ota, Ogun State, Nigeria. [d]Department of Physics, Mountain Top University, Ibafo, Ogun State, Nigeria.
[e]Division of Computational Physics, Institute for Computational Science, Ton Duc Thang University, Ho Chi Minh City, Vietnam [f]Faculty of Electrical and Electronics Engineering, Ton Duc Thang University, Ho Chi Minh City, Vietnam Corresponding author email: dilip.de@covenantuniversity.edu.ng

Abstract
Thermionic energy converter (TEC) has recently received significant attention, for it holds potential for clean energy generation with a very high theoretical conversion efficiency (60%). For the latter to be achieved, some of the key hurdles are to be overcome. This paper discusses all these key hurdles along with modelling of solar energy conversion using a TEC with nano-materials and metals, using the modified Richardson-Dushman equation, which best describes the thermionic emission current density from these materials. Using two scenarios: allowing natural heat radiation from the back surface of the collector and using controlled heat collection from the collector to maintain it at a fixed temperature. We then discuss results of simulation of the conversion efficiency as a function of temperatures of emitter and collector, work functions and Fermi energy of emitter and collector at absolute zero temperature, solar insolation, the radius of parabolic concentrator and emissivity of radiating surfaces. We discuss the impact of neglecting the radiation losses on the efficiency evaluation as has been done by other workers recently. We suggest some innovative ways to reduce significantly the space charge effect to make a solar TEC a reality.

Keywords: Thermionic energy converter; solar energy; modelling; modified Richardson-Dushman equation; metals; nanomaterials; high conversion efficiency; clean energy, parabolic concentrator.

1.   Introduction

Significant research interest is currently focused on the thermionic conversion of heat energy to electrical energy/power using thermionic energy converter (TEC), because like solar PV, TEC offers a very clean energy generation technique with absolutely no pollution [1,2]. However, unlike solar PV, TEC has a special advantage of giving very high output power density (per unit area of TEC active surface) [2,3]. No power converter can match TEC in output power density, making it most ideal for space application [3,4]. It uses the principle of thermionic emission of electrons from a heated solid surface (below the melting point). The thermionic current density J at temperature T(K) is, in general, guided by Richardson-Dushman's (RD) equation [5–7].

$$J = A_0 T^2 \exp(-W/k_B T) \qquad (1)$$

Hence, W is the work function of the emitter, k_B is the Boltzmann constant. The emitted electrons, when collected by a colder anode (collector), constitutes electrical current that can drive a load in Figure 1 [8].
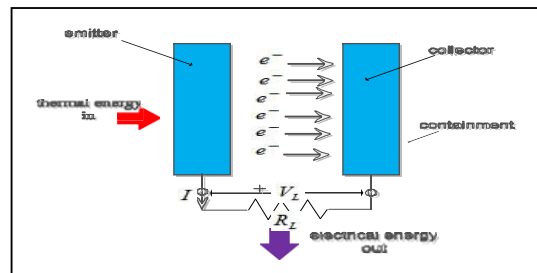
Figure 1: Schematic diagram of the thermionic energy converter [8]

In the next section, we consider (i) new development in TEC (ii) reduction of space charge effect (iii) principle of thermionic energy converter TEC and the use of graphene as emitter and collector; (iv) theory of the solar TEC and finally we present our own works on solar thermionic energy conversion efficiency with graphene as emitter and collector

2   New development in TEC

Solar thermionic power generation is currently receiving attention [3,4,9–12]. The SLAC/Stanford University research team is creating a new solid-state energy conversion technology based on micro-fabricated heterostructure semiconductor cathodes with appropriate band engineering and photon-enhanced thermionic energy converters (PETECs)[8,12]. The microfabrication allows a very small gap (a few microns) between the emitter and collector and thus reduces the space charge effect drastically. When used as a topping cycle in concentrated solar thermal electricity generation, PETECs is expected to enable total system efficiencies in excess of 50%. However, a practical device has not yet been realized using PETEC and micromachined is discussed also below.

Solar TEC is promising for future use as a topping cycle in concentrated solar thermal and in concentrated photovoltaic stations. However, to our knowledge, a practical solar TEC has not been realized yet. Recently, theoretical research has been focused on modelling solar TEC where solar energy is concentrated onto the emitter surface by a parabolic concentrator [3,10,14]. The latest work in this direction shows for the first time the importance and method of controlling the collector temperature in a solar TEC. This is important to achieve the desired efficiency after the space charge effect is reduced by the architectural combination of magnetic field and electrode gates.

Many emitter materials have work functions in the range of 3 to 4.5 eV. These require very high temperature (above 2000 K) to generate notable current density. Except for a few refractory metals (such as Tungsten), most materials have a melting point below 2000 K and therefore not suitable for high-temperature TEC. Even though intensive researches are being conducted to lower the work function of materials, they are still at a developmental stage for application to TEC. Tungsten and graphene are special materials for TEC since both have high melting points. For higher efficiency of TEC, it is important that the emitters should have a high melting point since efficiency increases with the temperature of operation. In places where sunshine is abundant, like in many Asian and African countries and parts of USA, high temperature at a small area of the emitter (1- 4 cm^2) can be created using parabolic concentrator.

Nanomaterials (emitters) with a high melting point are receiving attention for the conversion of the thermal energy to electrical power by thermionic energy converters (TECs) [8,15]. The addition of electrostatic gating method with a Cs/O surface coating on large area monolayer graphene grown by chemical vapour deposition and then transferring onto 20 nm HfO_2 on Si that enables high electric fields capacitive charge accumulation in the graphene, as to reduce the work function of graphene from 4 $4.6\ eV\ to\ 0.7\ eV$ [15]. Such ultra-low work function graphene is an ideal candidate for graphene as the thermionic emitter in TEC, specifically, for low-temperature

TEC [16]. Liang *et al.* [17] proposed and theoretically studied a solid state thermionic device comprising of van der Waals heterostructures of suitable multiple layers of transition metal dichalcogenides such as MOS_2, $MOSe_2$, WS_2 and WSe_2 sandwiched between two graphene electrodes to waste heat at 400 K and found efficiencies in the range of 7% to 8%. Being a high-temperature material, graphene is a suitable material for thermionic energy conversion, specifically, if the work function of graphene can be reduced from around $4.5\ eV$ to around $1.5\ eV$, using some of the technologies as mentioned above [18]. Technologies have been maturing for growth of mono to multilayers of graphene (Gr) on silicon carbide [19,20]. The latter is a material that also can sustain high temperature. Epitaxial Gr on silicon carbide (SiC) holds great promise for the development of new device concepts based on the vertical current transport at Gr/SiC hetero-interface [21]. Work function modulation of graphene on SiC has also been obtained recently through the controlled use of nitric acid [21]. Recently Kwon *et al.* (2012) [22] reported a chemical approach to the lower work function of graphene using K_2CO_3, Li_2CO_3, Rb_2CO_3, Cs_2CO_3. The work functions are reported to be 3.7 eV, 3.8 eV, 3.5 eV and 3.4 eV. Such remarkable property along with good electrical conductivity, high dielectric constant makes engineered graphene an ideal candidate to be used as both emitter and collector in a thermionic energy converter.

Graphene has distinguished itself from semiconductor and the other nanomaterials due to superior properties in the linear band structure, ultrahigh electrical conductivity, high stiffness light weight and extreme mobility [23]. Graphene emitter, therefore, is as a good candidate for the thermionic engine. It has its place because of the presence of free electron in the linear band structure, which is in proximity to Fermi level, that is deficient in macro material [24–29]. Alteration in the chemical potential across the graphene sheet provides room to tuning the intrinsic Fermi level (Chemical potential, μ) to corresponding Dirac point by choice of the investigator [30], and thus the work function W $(W = E_v - \mu)$, . Graphene has attractive features and a lot of applications in nano-electronics [31,32] energy storage [33], and composites [34]. Thus, graphene can become the ideal candidate for thermionic power generation with the use of solar concentrators as shown in Figure 3a. Thus, it is expected that with the advent of new science and technology, several layers of graphene on silicon carbide can be deposited such that work function can be controlled at ease from around $4.6\ eV$ to around $0.7\ eV$, as desired, while retaining its high-temperature tolerance.

2.1   Reduction of space charge effect

Space charge is formed in between the emitter and collector space (which is to be maintained at vacuum and may be filled with positive caesium ions) when all the emitted electrons from emitter could not be collected by the anode simultaneously.

In recent time, a revolutionary modification of TEC was proposed and demonstrated. Simply by filling in the inter-electrode gap of the TEC with a nanofluid, which consist of gold nanoparticles dispersed in tetradecane base fluid, Nguyen *et. al.* [13] removed most of the aforementioned limitations and introduced many advantages toward further potential applications of TECs. In addition to direct thermionic emission from the cathode to the anode, this modification added an indirect charge transport channel via the nanoparticles Firstly, by changing from the gas phase to fluid phase, the space charge effect is reduced naturally. Secondly, by interactions with the nanoparticles that form temporary potential barriers for nano-hopping or tunnelling of electrons, the escape energy (work function) of any cathode material can be effectively lowered. Moreover, the requirement of the high-temperature contrast between cathode and anode can be tolerant; and the output current density of a nanofluid TEC was demonstrated to be strongly enhanced. However,

because the theoretical platform for this new concept is still under developing, further discussion on its theory is outside the scope of this paper. The nanofluid device is of course benefit from new developments that will be discussed next in this review paper.

These space charges can be minimized by (i) keeping the separation between emitter and collector of the order of micron; (which is very difficult while maintaining a significant temperature difference between the two electrodes), (ii) applications of the magnetic field, and gate voltage (Figure 2c). The latter is an innovative technique shown to be effective[6]. Guided by accelerating electric field and cycloidal path motion in the magnetic field, the electron scattering is reduced significantly. The diameter of the holes in the gate must be such that (i) it allows fairly uniform electric field directed normal to the emitter; (ii) while maximizing the hole space in the gate as much as possible (to minimize gate current), (iii) it should be slightly larger than the cyclotron radius of most electrons. A high magnetic field can accomplish the latter [3,10,14].

In particular, this scientific work jettisons the effect of space charge in the TEC. Partial space charge neutrality could be accomplished as shown in Figures (2b and 2c) together with the following criteria: Nanoengineering could be adopted to configure the emitter in a pencil-like manner with height $0.5\ mm$ and diameter $0.7\ \mu m$. For a total collection of emitted electrons approximately 99.8 % on collector plate, there is a need to insert a gate electrode with diameter holes $1-1.5\ mm$ at an approximate distance $0.7-1.0\ mm$ in between the emitter and collector. Consequentially, the diameter hole of the gate should double the radius of the cyclotron $rrcc$ of the liberated electron. Hence the mean free path of the liberated electron is expressed as
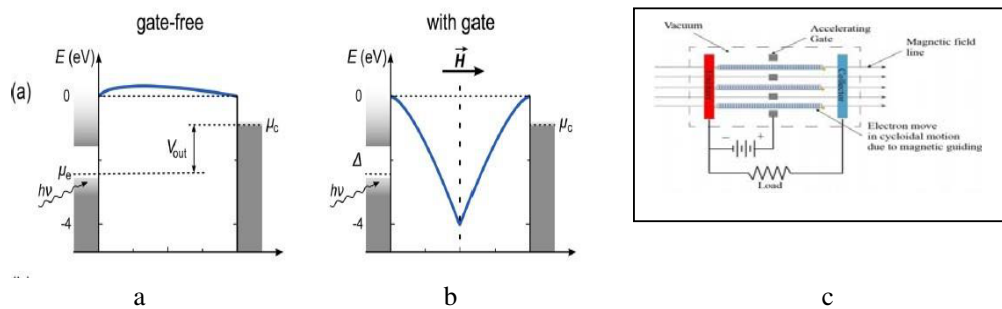
$$mv_m = Ber_c \qquad (2a)$$

Figure 2: (a) shows that the work function W of the emitter is greater than that of the collector in the absence of gate at the inter-electrode. The difference is equal to about. (b) insertion of a positive gate between the cathode and collector, with a hole of radius R and a magnetic field at a right angle to the gate towards the collector [4] (c) reduction of space charge effect in TEC via the inclusion of gate and magnetic field [4,35]

$$\tfrac{1}{2}mv_m^2 = 2k_B T_e \qquad (2b)$$

where v_m is the mean velocity of the emitted electrons, m is the electron mass and k_B is the Boltzmann's constant and r_c typifies the radius.

3   Principles of Thermionic Energy Converter (TEC)

The principle of thermionic energy conversion has been explained lucidly in [8]. The output power in a TEC (Fig.3),

$$P_{out} = \frac{(I_e - I_c)(W_e - W_c)}{e} \tag{3a}$$

$$P_{out} = \frac{s(J_e - J_c)(W_e - W_c)}{e} \tag{3b}$$

where I_e is the emitter current and I_c is the collector current. s is the area of emitter which is equal to that of the collector in this modelling. Again, the separation between emitter and collector has to be very small to reduce the space charge effect (discussed earlier), specially, in absence of gate and magnetic field control (discussed earlier) so that, the electric field $(E = \Phi/d)$ is strong to pull the emitted electrons fast onto the collector, in order to minimize the space charge problem. The space charge will affect the net output power.

The emitter and collector current density and J_e depend J_c not only on emitter and collector temperatures TT_{ee}, TT_{cc}, their work functions WW_{ee}, WW_{cc}, the distance between the two plates but also arrangements that control space charge. The accuracy of the modified Richardson-Dushman Equation in predicting the current density of graphene and carbon nanotube over Richardson Equation and Liang and Ang[27] model has been reported [36,37].

In addition, Figure 3a shows how the centre of the cathode-anode configuration is positioned on the axis of the parabolic concentrator and at a right angle to it. In order, to allow all the solar irradiation to be concentrated on the emitter in Figure 3a, the cathode-anode configuration must be strategically placed at a height h. Also, a nanoscale coating could be done for more absorption and low reflection of solar irradiation on the surface 1 of Figure 3b.

Moreover, we assume that large size (2- 6 m diameter) parabolic concentrators may be possible one day and that the graphene emitter (on silicon carbide) of the TEC is placed on the axis of the parabolic concentrator [Figure 3a]. We assume that a magnet can be attached with its south pole on the collector and the magnet can be cooled at a rate Q_r. We then consider the energy exchange processes that take place in such a graphene TEC and compute the efficiency of the graphene TEC for various parameters such as, solar insolation, anode temperature, diameter of parabolic mirror, emitter height (which determines the effective emitter cross-section) from the base of the mirror, mirror reflection coefficients etc. To our knowledge, such a theoretical concept of computation of efficiency of graphene TEC has not been applied by other workers and it is different from those discussed earlier in a different model [3,10,14]. The calculation of efficiency in a TEC by other workers so far has excluded radiation heat losses and energy conservation processes [38]. In this paper, we have considered graphene surfaces on SiC and assumed that the graphene surfaces can be suitably engineered for work functions to be used as emitter and collector in a solar TEC. We shall not dwell on the space charge effect that limits the power put from a TEC. This thermionic energy converter reduces the dependence on silicon and has the potential to charge a battery that can be used during off-peak of sunshine.
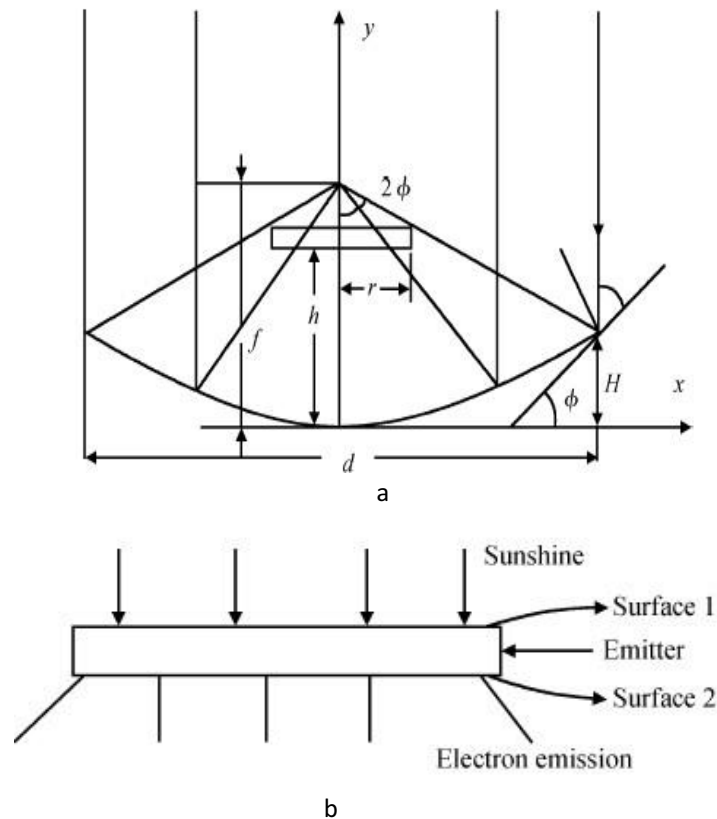
Figure 3: (a) Dependence of f upon [8,14,39] (b) Nanoscale coating of TEC plate [8,14]

The relationship that exists among radius r, height h and emitter area s, parabolic height H, parabolic radius R, the angle ϕ the parabolic mirror makes with its base and the focal length f of parabolic concentrator can be expressed mathematically as[14]:

$$tan\phi = H/2R \tag{4}$$

$$r = (f - h)tan2\phi \tag{5}$$

$$f = R^2/4H \tag{6}$$

4   Theory of the solar TEC

An electron emitted from the emitter at temperature T_e will require net average energy of $(W_e + 2k_BT_e)/e$. Solar energy I_0S is concentrated by the parabolic mirror on to the emitter of area s (surface 1 in Figure 3b). S is the area of the circular cross-section of the mirror (Figure 3a). The electron emission takes place from the second surface of the emitter. This can be achieved by covering the first surface with a thin quartz encapsulation and making the work function of the second surface somewhat lower than the first surface. Even if that is done, the first step should suffice to prevent continuous electron emission from the first surface. Then energy conservation demands that the following equation holds:

$$I_0S = \left[\frac{J_es(W_e+2k_BT_e)}{e} - \frac{J_cs(W_c+2k_BT_{1c})}{e}\right] + [\sigma s(T_{1e}^4 - T_a^4) + \sigma s(T_{2e}^4 - T_{1c}^4)] \tag{7}$$

In Equation (7) T_{1e}, T_{2e} and T_{1c} are respectively the temperatures of the first, second surfaces of the

emitter and the first surface of the collector. The first surface of collector's faces and collects the electrons emitted from the second surface of the emitter.

Here J_c is the collector current density. As discussed above collector work function. The efficiency η of solar power conversion is then given by:

$$\eta = \frac{(J_e - J_c)(W_e - W_c)}{\left[\frac{J_e s(W_e + 2k_B T_e)}{e} - \frac{J_c s(W_c + 2k_B T_{1c})}{e}\right] + \left[\sigma s(T_{1e}^4 - T_a^4) + \sigma s(T_{2e}^4 - T_{1c}^4)\right]} \tag{8}$$

From Equation (8) alone it is not possible to know T_e and T_c with known values of I_0, S, W_e and W_c. Considering the dynamics of energy exchange processes that take place in a solar TEC (Figure 3) the   following   equations   hold   for   the

$$\frac{k_e(T_{1e} - T_{2e})}{x_1} = J_e(W_{2e} + 2k_B T_{2e})/e + \sigma \varepsilon_e(T_{2e}^4 - T_{1e}^4) \quad \text{emitter of thickness } x_1 \text{ [8,14]:}$$

$$\sigma \varepsilon_e(T_{2e}^4 - T_{1c}^4) - J_c(W_c + 2k_B T_{1c})/e = \frac{k_e(T_{1e} - T_{2e})}{x_1} \tag{9}$$

$$\frac{k_e(T_{1e} - T_{2e})}{x_1} = \sigma \varepsilon_c(T_{2c}^4 - T_a^4) \tag{10}$$

$$\tag{11}$$

$$J = A_0 T^2 \exp\left(-\frac{\left[W_0 + r\alpha T E_{F_0} + \left(\begin{array}{c}(1+r\alpha T)\left(\frac{\pi^2}{12}\right)\left(\frac{k_B T}{E_{F_0}}\right)^2 (E_{F_0}) \\ +(1+r\alpha T)\left(\frac{7\pi^2}{960}\right)\left(\frac{k_B T}{E_{F_0}}\right)^4 (E_{F_0})\end{array}\right)\right]}{k_B T}\right) \tag{12}$$

where $r = 3$ for bulk material or thick surface and $r = 2$ for a 2-D thin surface. Now we see from Eqs. (1)-(12), which provides an ideal model for a solar TEC, that it is a non-trivial job to solve analytically for T_{1e}, T_{2e}, T_{1c} and T_{2c} hence Equation (8) for the efficiency of the solar TEC.

In this paper, we want to study particularly the effect of work function and temperature of the collector in the efficiency of a solar TEC, keeping *We* (work function of the emitter) fixed at high value of 4.5 eV. This value is close to the work function of tungsten and graphene without any surface work to reduce the work function. In so doing, we want to simplify the model by assuming both emitter and collector to be thin enough so that these can be characterized by temperatures,

$$T_e = \left(\frac{T_{1e} + T_{2e}}{2}\right) \tag{13}$$

$$T_c = \left(\frac{T_{1c} + T_{2c}}{2}\right) \tag{14}$$

Then Equations (8 and 9) can be written as:

$$I_0 S = \left[\frac{J_e s(W_e + 2k_B T_e)}{e} - \frac{J_c s(W_c + 2k_B T_c)}{e}\right] + \left[\sigma s(T_e^4 - T_a^4) + \sigma s(T_e^4 - T_{1c}^4)\right] \tag{15}$$

$$\eta = \frac{(J_e - J_c)(W_e - W_c)}{\left[\frac{J_e s(W_e + 2k_B T_e)}{e} - \frac{J_c s(W_c + 2k_B T_c)}{e}\right] + \left[\sigma s(T_e^4 - T_a^4) + \sigma s(T_{2e}^4 - T_c^4)\right]} \tag{16}$$

In this simulation, we assume two parabolic concentrators with a circular aperture of radius $r = 1\,m$ and $r = 2\,m$; As high temperature is needed to obtain good efficiency, the cross-section of the emitter has to be small. We choose two emitter cross sections in these simulations: $s = 0.0001\,m^2$; $s = 0.0002\,m^2$. Assuming $T_c = 373\,K$, Tables 1 and 2 show simulated efficiency of TEC in the absence space charge problem and $100\,\%$ reflection coefficient of the parabolic mirror and $100\,\%$ absorption coefficient of the emitter surface for the reflected and concentrated solar light energy.

Table 1: Simulated efficiency for various solar insolation with parabolic concentrator of radius $R = 1\,m$ with $T_c = 373\,K$ for emitter cross section $s = 0.0002\,m^2$ MRD Model

R(m)	I_0= 500 W/m2	I_0= 600 W/m2	I_0= 700 W/m2	I_0= 800 W/m2	I_0= 900 W/m2	I_0= 1000 W/m2
1	22.2	22.6(1764)	23	23.4	23.6	23.8(1838)
2	25.1	25.4(1974)	25.7	25.9	26.1	26.3(2064)

Table 2: Simulated efficiency for various solar insolation with parabolic concentrator of radius $R = 1\,m$ with $T_c = 1073\,K$ for emitter cross section $s = 0.0002\,m^2$ MRD model

R(m)	I_0= 500 W/m2	I_0= 600 W/m2	I_0= 700 W/m2	I_0= 800 W/m2	I_0= 900 W/m2	I_0= 1000 W/m2
1	21	21.5(1768)	21.8	22.2	22.4	22.7(1840)
2	23.9	24.2(1974)	24.5	24.7	24.9	25(2064)

Table 3: Simulated efficiency for various solar insolation with parabolic concentrator of radius $R = 1\,m$ with $T_c = 373\,K$ for emitter cross section $s = 0.0001\,m^2$, $W_e = 2\,eV$ and $W_c = 1.5\,eV$ MRD model

R(m)	I_0= 500 (W/m^2)	I_0= 600 (W/m^2)	I_0= 700 (W/m^2)	I_0= 800 (W/m^2)	I_0= 900 (W/m^2)	I_0= 1000 (W/m^2)
1	23.8	24.2(1864)	24.5	24.7	24.9	25(1944)
2	26.2	26.6(2098)	26.8	27.0	27.2	27.4(2200)

Table 4: Simulated efficiency for various solar insolation with parabolic concentrator of radius $R = 1\,m$ with $T_c = 1037\,K$ for emitter cross section $s = 0.0001\,m^2$, $W_e = 2\,eV$ and $W_c = 1.5\,eV$ MRD model

R(m)	I_0= 500 (W/m^2)	I_0= 600 (W/m^2)	I_0= 700 (W/m^2)	I_0= 800 (W/m^2)	I_0= 900 (W/m^2)	I_0= 1000 (W/m^2)
1	22.6	23.0(1866)	23.3	23.5	23.7	23.9(1944)
2	25.0	25.4(2096)	25.6	25.8	26.0	26.2(2200)

Table 5: Simulated efficiency for various solar insolation with parabolic concentrator of radius $R = 1\,m$ with $T_c = 373\,K$ for emitter cross section $s = 0.0001\,m^2$, $W_e = 2\,eV$ and $W_c = 1.5\,eV$ RD model

R(m)	I_0= 500 (W/m^2)	I_0= 600 (W/m^2)	I_0= 700 (W/m^2)	I_0= 800 (W/m^2)	I_0= 900 (W/m^2)	I_0= 1000 (W/m^2)

| 1 | 22.6 | 23.0(1866) | 23.3 | 23.5 | 23.7 | 23.9(1944) |
| 2 | 25.0 | 25.4(2096) | 25.6 | 25.8 | 26.0 | 26.2(2200) |

Table 6: Simulated efficiency for various solar insolation with parabolic concentrator of radius $R = 1\,m$ with $T_c = 373\,K$ for emitter cross section $s = 0.0001\,m^2$, $W_e = 2\,eV$ and $W_c = 1.5\,eV$ MRD model

R(m)	$I_0 = 500$ (W/m²)	$I_0 = 600$ (W/m²)	$I_0 = 700$ (W/m²)	$I_0 = 800$ (W/m²)	$I_0 = 900$ (W/m²)	$I_0 = 1000$ (W/m²)
1	42.5(1838)	42.9(1864)	43.4	43.6	44.2	44.1(1944)
2	45.24(2064)	45.5(2098)	45.7	45.9	46.0	46.2(2200)

5   Discussion

From the above tables the following facts emerge for MRD model:

i. Efficiency increases slightly at higher solar insolation when all other parameters are held constant

ii. With higher diameter (radius) of the parabolic concentrator, the efficiency is higher for the same solar insolation.

iii. The emitter temperature T_e at which energy balance occurs increases with solar insolation and radius of parabolic concentrator when T_c, W_e, W_c are held constant.

iv. Even though efficiency increases with the decrease of collector temperature, it decreases with higher emitter cross section for the same parabolic mirror.

Table 5 shows efficiency simulation for various solar insolation with $s = 1$ and $R = 1 \text{ and } 2\,m$ for $W_e = 2\,eV$, $W_c = 1.5\,eV$ and $T_c = 373\,K$ with the RD model. It is seen that though the RD model gives thermionic efficiency slightly less than the MRDE model in Table 3, the temperature at which energy balance occurs remains the same as with the RD model. Table 6 shows the effect of the reduction of the work function of the collector. This increases the output potential from $0.5\,eV$ in the earlier cases (Tables 1-5) to $1\,eV$ (Table 6) for $T_c = 373\,K$. We see a dramatic increase in efficiency.

However, the temperature Te at which energy balance occurs in Equation 15 for various solar insolation I_0 remains essentially the same as in Tables 1-5. T_e as before increases with radius of parabolic mirror and insolation for a mirror of a given radius. Efficiency at a given Te depends on many factors but critically on W_e and W_c. For high efficiency of thermionic power conversion, it is essential that the values of these two important quantities should be as low as possible while the difference is greater than $0.5\,eV$. It is for this reason significant research is being currently devoted to the discovery of materials of low work function [21,22,40,41].

6   Conclusion

Based on our above simulation it is understandable that if the space charge problem can be fully controlled and collector temperature can be adjusted using controlled heat extraction method discussed later, the study can obtain high efficiency of thermionic solar energy conversion. Even if space charge is not fully controlled, good efficiency of conversion is possible if large size parabolic concentrator can be obtained and materials can be fabricated that can stand high temperature while possessing low work function at the surface of electron emission.

To generate a sizable amount of electrical power (several kW) from the sun using thermionic converter one needs large size parabolic concentrators[17]. The parabolic concentrator of diameter ~2.6 feet costs around $200. It is expected that large size parabolic mirror (imaging type) of diameter $4\,m$ to $6\,m$ can be purchased at a cost of around $1500-2000. Then cost-effective solar thermionic power conversion would be possible, as it can generate high temperature onto a small surface to produce very high emission current density.

References

[1]   Strohl, G. R., & Sissom, L. E. Thermionic power converter | electronics | Britannica.com

[2]   Chao, J. (2016). Scientists Look to Thermionic Energy Conversion for Clean and Efficient Power Generation

[3]   De, D. K. & Olukunle, O. C. (2015). A Theoretical Study on Solar Thermionic (thermo electronic) Power Conversion with a Parabolic Concentrator

[4]   Meir, S., Stephanos, C., Geballe, T. H., & Mannhart, J. J. (2013). Highly-Efficient Thermoelectronic Conversion of Solar Energy and Heat into Electric Power *Journal Renewable, Sustainable Energy,* **5**: 1-27.

[5]   Richardson, O. W. (1913). The emission of Electrons from Tungsten at High Temperatures: an Experimental Proof that the Electric Current in Metals is Carried by Electrons. *Science, (80)***38,** 57–61.

[6]   Richardson, O. (1901). *On the Negative Radiation from Hot Platinum. Cambridge Philosophical Society*, 11, 286.

[7]   Richardson O W Thermionic phenomena and the laws which govern them

[8]   Olawole, O. C., & De, D. K. (2018). Theoretical Studies of Thermionic Conversion of Solar Energy with Graphene as Emitter and Collector. *Journal of Photonics Energy,* (**8)1,** 1-27.

[9]   Harper, J. (2002). How vacuum tubes really work *2-01-2002*

[10]   Olawole, O. C., De, D. K., & Oyedepo, S. O. (2016). Energy Dynamics of Solar Thermionic Power Conversion with Emitter of Graphene. *Proc. SPIE,* **9932**, 1-7.

[11]   Schwede J W, Sarmiento T, Narasimhan V K, Rosenthal S J, Riley D C, Schmitt F, Bargatin I, Sahasrabuddhe K, Howe R T, Harris J S, Melosh N A and Shen Z-X 2013 PhotonEnhanced Thermionic Emission from Heterostructures with Low Interface Recombination *Nat. Commun.* **4** 1576

[12]   Kribus, A., & Segev, G. (2016). Solar Energy Conversion with Photon-Enhanced Thermionic Emission *J. Opt.* **18** 073001

[13]   Nguyễn, H. M., Lu, J., Goto, H. & Maeda, R. (2018). Thermionic Emission via a Nanofluid for Direct Electrification from Low-Grade Heat Energy. *Nano Energy,* **49,** 172–178.

[14]   Olukunle, O. C., & De, D. K. (2016). Thermo-Electronic Solar Power Conversion with a Parabolic Concentrator. *Journal of Semiconductor,* **37** 024002

[15]   Yuan, H., Riley, D. C., Shen, Z. X., Pianetta, P. A., Melosh, N. A., & Howe, R. T. (2017). Back-Gated Graphene Anode for More Efficient Thermionic Energy Converters. *Nano Energy,* **32**, 67–72.

[16]   Misra, S., Upadhyay-Kahaly, M., & Mishra, S. K. (2017). Thermionic Emission from Monolayer Graphene, Sheath Formation and its Feasibility Towards Thermionic Converters. *Journal of Applied Physics,.* **121,** 065102

[17]   Liang, S. J., Liu, B., Hu, W., Zhou, K., & Ang, L. K. (2017). Thermionic Energy Conversion Based on Graphene van der Waals Heterostructures *Scientific Report,* **7,** 46211

[18]   Yin, Y., Cheng, Z., Wang, L., Jin, K., & Wang, W. (2015). Graphene, a Material for High Temperature Devices – Intrinsic Carrier Density, Carrier Drift Velocity and Lattice Energy *Scientific Report,* **4**, 5758

[19]   Juang, Z. Y., Wu, C. Y., Lo, C. W., Chen, W. Y., Huang, C. F., Hwang, J. C., Chen, F. R., Leou, K. C., & Tsai, C. H. (2009). Synthesis of Graphene on Silicon Carbide Substrates at Low Temperature. *Carbon,* **47,** 2026–3201

[20]   Mishra, N., Boeckl, J., Motta, N., & Iacopi, F. (2016). Graphene Growth on Silicon Carbide: A Review. *Physics Status Solidi,* **213,** 2277–2289.

[21]   Giannazzo, F. (2016). Insight into the Mechanisms of Chemical Doping of Graphene on Silicon Carbide. *Nanotechnology,* **27,** 072502

[22] Kwon, K. C., Choi, K. S., Kim, B. J., Lee, J. L, and Kim, S. Y. (2012). Work-Function Decrease of Graphene Sheet Using Alkali Metal Carbonates. *J. Phys. Chem. C* **116** 26586– 91

[23] Rao, C. N. R., Chintamani N. R., Sood, A. K., & Ajay, K. (2013). Graphene : Synthesis, Properties, and Phenomena. *Wiley*

[24] Sun, S., Ang, L. K., Shiffler, D., & Luginsland, J. W. (2011). Klein Tunnelling Model of Low Energy Electron Field Emission from Single-Layer Graphene Sheet *Applied Physics Letter,* **99** 013112

[25] Wei X, Golberg D, Chen Q, Bando Y, Peng L 2011 Phonon-Assisted Electron Emission from Individual Carbon Nanotubes *Nano Letters,* **11,** 734–739.

[26] Liang, S. J., Sun, S., Ang, L. K. (2013). Over-Barrier Side-Band Electron Emission from Graphene with a Time-Oscillating Potential. *Carbon,* **61,** 294–298.

[27] Liang, S. J. & Ang, L. K. (2014). Chiral Tunneling-Assisted Over-Barrier Electron Emission From Graphene. *IEEE Transaction Electron Devices,* **61,** 1764–1770.

[28] Wei, X., Wang, S., Chen, Q. & Peng, L. (2015). Breakdown of Richardson's Law in Electron Emission from Individual Self-Joule-Heated Carbon Nanotubes. *Scientific Reports* **4** 5102

[29] Craciun, M. F., Russo, S., Yamamoto, M., & Tarucha, S. (2011). Tuneable Electronic Properties in Graphene

[30] Novoselov, K. S., Geim, A. K., Morozov, S. V., Jiang, D., Zhang, Y., Dubonos, S. V., Grigorieva, I. V, Firsov, A. A. (2004). Electric Field Effect in Atomically Thin Carbon Films. *Nature,* **306** 666

[31] Wei Z Q 2010 Nanoscale tunable reduction of graphene oxide for graphene electronics *Science (80-.).* **328** 1373–6

[32] Lee S, Lee K, Zhong Z 2010 Wafer Scale Homogeneous Bilayer Graphene Films by Chemical Vapor Deposition *Nano Lett.* **10** 4702–7

[33] Liu C, Yu Z, Neff D, Zhamu A, Jang B Z 2010 Graphene-Based Supercapacitor with an Ultrahigh Energy Density *Nano Lett.* **10** 4863–8

[34] Stankovich S, Dikin D A, Dommett G H B, Kohlhaas K M, Zimney E J, Stach E A, Piner R D, Nguyen S T, Ruoff R S 2006 Graphene-based composite materials *Nature* **442** 282–6

[35] Wanke R, Hassink G W J, Stephanos C, Rastegar I, Braun W, Mannhart J 2016 Magnetic-Field-Free Thermoelectronic Power Conversion Based on Graphene and Related TwoDimensional Materials *J. Appl. Phys.* **119**

[36] Olawole O C, De D K. Modeling thermionic emission from carbon nanotubes with modified Richardson-Dushman equation[J]. SPIE,2016, 992716

[37] De D K, Olawole O C 2016 Modified Richardson–Dushman equation and modeling thermionic emission from monolayer graphene *Proc. SPIE* **9927**, 1-8

[38] Starodub E, Bartelt N C, Mccarty K F Viable thermionic emission from graphene-covered metals[J]. *J. Phys. Lett.,* 2012, **100** (18) 1-5

[39] De D K, Olukunle O C 2015 A brief review of solar concentrators[J]. *International Conference on Energy Economics and Environment (ICEEE)* (IEEE), 2015, pp 1–7 [40] Paxton W F, Wisitsoraat A, Raina S, Davidson J L, Kang W P. 2010 P2.14: Characterization of the thermionic electron emission properties of nitrogen-incorporated "ridged" nanodiamond for use in thermal energy conversion *International Vacuum Nanoelectronics Conference* (IEEE) pp 149–150

[41] Yuan H, Chang S, Bargatin I, Wang N C, Riley D C, Wang H, Schwede J W, Provine J, Pop E, Shen Z-X, Pianetta P A, Melosh N A, Howe R T 2015 Engineering Ultra-Low Work Function of Graphene *Nano Lett.* **15** 6475–80